Finite-size and pressure effects in $YBa_2Cu_4O_8$ probed by magnetic-field penetration-depth measurements

R. Khasanov,[1,2,3,*] T. Schneider,[3] R. Brütsch,[4] D. Gavillet,[4] J. Karpinski,[5] and H. Keller[3]
[1]*Laboratory for Neutron Scattering, ETH Zürich and Paul Scherrer Institut, CH-5232 Villigen PSI, Switzerland*
[2]*DPMC, Université de Genève, 24 Quai Ernest-Ansermet, 1211 Genève 4, Switzerland*
[3]*Physik-Institut der Universität Zürich, Winterthurerstrasse 190, CH-8057, Switzerland*
[4]*Laboratory for Material Behaviour, Paul Scherrer Institut, CH-5232 Villigen PSI, Switzerland*
[5]*Solid State Physics Laboratory, ETH 8093 Zürich, Switzerland*
(Received 11 January 2004; revised manuscript received 7 May 2004; published 22 October 2004)

We explore the combined pressure and finite-size effects on the in-plane penetration depth λ_{ab} in $YBa_2Cu_4O_8$. Even though this cuprate is *stoichiometric* the finite-size scaling analysis of $1/\lambda_{ab}^2(T)$ uncovers the *granular nature* and reveals domains with nanoscale size L_c along the *c*-axis. L_c ranges from 50.8 (1.0)Å to 39.3 (8)Å at pressures from 0.0 to 10.2 kbar. These observations raise serious doubts on the existence of a phase coherent macroscopic superconducting state in cuprate superconductors.

DOI: 10.1103/PhysRevB.70.144515 PACS number(s): 74.72.Bk, 74.62.Fj, 74.25.Ha, 83.80.Fg

I. INTRODUCTION

There is increasing evidence that inhomogeneities are an intrinsic property of cuprates (see, e.g., Ref. 1 and references therein). Studies of different cuprate families revealed the segregation of the material in superconducting and nonsuperconducting regions. In particular, neutron scattering,[2] electron paramagnetic resonance (EPR),[3] scanning tunneling microscopy (STM),[4] and x-ray diffraction[5] provide evidence for granular superconductivity in the cuprates. Although crystals of the cuprates are not granular in a structural sense, it occurs when microscopic superconducting domains are separated by nonsuperconducting regions through which they communicate for instance by Josephson tunneling to establish the macroscopic superconducting state.

On the other hand, there is evidence for nearly isolated, homogeneous and superconducting domains of nanoscale extent embedded in a nonsuperconducting matrix.[1,6–8] It stems from a finite-size scaling analysis of the thermal fluctuation contributions to the specific heat[6] and magnetic field penetration depth data.[1,7,8] In an isolated domain there is a finite-size effect because the correlation length cannot grow beyond the length of the superconducting domain in direction *i*. Accordingly there is no sharp phase transition and the specific heat coefficient will exhibit a blurred peak with a maximum at $T_p < T_c$, where T_c is the transition temperature of the homogeneous bulk system. At T_p the correlation length $\xi(T)$ reaches the limiting length L of the domain. Similarly, $1/\lambda^2$, where λ is the magnetic field penetration depth, does not vanish at T_c, but exhibits a tail with an inflection point at T_p. This raises serious doubts on the existence of macroscopic phase coherent superconductivity, suggesting that bulk superconductivity is achieved by a percolative process. Therefore, superconducting properties and the spatial extent of the domains can be probed by thermal fluctuations and the finite-size effects. This includes the effects of oxygen isotope exchange and pressure on the domain size. Recently a significant change of spatial extent of the superconducting domains upon oxygen isotope exchange has been demonstrated in $Y_{1-x}Pr_xBa_2Cu_3O_{7-\delta}$.[7] It revealed the relevance of local lattice distortions in the occurrence of superconductivity.

In this paper we address the pressure studies of the finite-size effect in $YBa_2Cu_4O_8$, which exhibits a rather large and positive pressure effect (PE) on T_c, with $dT_c/dp \simeq 0.50(1)$ K/kbar.[9–11] Even though this cuprate is *stoichiometric* the finite-size scaling analysis uncovers the existence of *nanoscale domains* with a spatial extent L_c along the crystallographic *c*-axis. The value of L_c decreases from 50.8(1.0) to 39.3(8) Å with increasing pressure from 0.0 to 10.2 kbar. Accordingly, T_c *increases* with *reduced thickness* L_c of the domains.

The paper is organized as follows. In Sec. II we sketch the finite-size scaling theory adapted for the analysis of penetration depth data. In Sec. III we describe the sample preparation procedure and the experimental technique, adopted to deduce the in-plane magnetic field penetration depth λ_{ab} from the Meissner fraction measurements. In Sec. IV we perform the finite-size analysis of the data for the in-plane magnetic penetration depth $\lambda_{ab}(T)$ taken at different pressures. Section V comprises the analysis of the pressure dependence of the domain lengths L_c along the crystallographic *c*-axis.

II. THEORETICAL BACKGROUND

The detailed description of the finite-size scaling theory adopted for the analysis of the magnetic field penetration depth λ can be found in Refs. 1, 6, and 7. Briefly, the main signatures for the existence of finite-size behavior appearing in the temperature dependence of the in-plane magnetic penetration depth λ_{ab} can be summarized as follows:[1]

(i) Denoting the spatial extent of the domains along the crystallographic a-, b- and *c*-axes with L_a, L_b and L_c, the transverse in-plane correlation lengths ξ_{ab}^t cannot diverge at $T=T_c$ but are limited by

$$\xi_{ab}^t(T) \leqslant L_c. \tag{1}$$

Consequently, for finite superconducting domains, the penetration depth is a smooth function of temperature. As a rem-

nant of the singularity at T_c, λ_{ab}^{-2} exhibits a so called finite-size effect,[1] namely an *inflection point* at T_{p_c} so that

$$\left.\frac{d\lambda_{ab}^{-2}(T)}{dT}\right|_{T=T_{p_c}} = extremum. \tag{2}$$

(ii) The absolute value of the superconducting domain size along the *c*-axis (L_c) can be estimated knowing λ_{ab} at $T=T_{p_c}$ as[1,6,7]

$$L_c \simeq \frac{16\pi^3 k_B T_{p_c} \lambda_{ab}^2(T_{p_c})}{\Phi_0^2}, \tag{3}$$

where Φ_0 is the flux quantum, and k_B is the Boltzmann's constant.

(iii) Apart from the inflection point, an essential characteristic of a finite size effect is the finite-size scaling function.[12] According to Ref. 1 it is defined in terms of

$$g(y) = \frac{\lambda_{0ab}^2}{\lambda_{ab}^2}|t|^{-\nu}, \tag{4}$$

where y is equal to

$$y = \mathrm{sign}(t)\left|\frac{t}{t_{pc}}\right|,$$

$t=T/T_c-1$, $t_{p_c}=T_{p_c}/T_c-1$, ν is the critical exponent, and λ_{0ab} is the critical amplitude.[1]

For the homogenous system ($L_c\to\infty$) and $t\neq 0$ ($y\neq 0$), $g(y)$ corresponds to the stepwise function

$$g_\infty(y<0)=1, \quad g_\infty(y>0)=0, \tag{5}$$

while for the system confined by the finite geometry ($L_c \neq 0$) the scaling function $g(y)$ diverges at $t\to 0$ ($y\to 0$) as

$$g(y\to 0) = g_{0c}y^{-\nu} = g_{0c}\left(\left|\frac{t}{t_{p_c}}\right|\right)^{-\nu}. \tag{6}$$

III. EXPERIMENTAL DETAILS

A. Sample preparation and characterization

The polycrystalline $YBa_2Cu_4O_8$ samples were synthesized by solid-state reactions using high-purity Y_2O_3, $BaCO_3$ and CuO. The samples were calcinated at 880–935 °C in air for 110 hours with several intermediate grindings. The phase-purity of the material was examined using a powder x-ray diffractometer. Only $YBa_2Cu_3O_{7-x}$ and CuO phases were revealed. The synthesis was continued at a high oxygen pressure of 500 bar, at 1000 °C during 30 hours. The x-ray diffraction measurements performed after the final stage of the synthesis revealed 95% of the $YBa_2Cu_4O_8$ phase. The sample was then reground in mortar for about 60 min and passed through the 10 μm sieve in order to obtain sufficiently small grains, as required for the determination of λ from Meissner fraction measurements. As it was shown in Ref. 13 the grounding procedure does not introduce any additional defects. The grain size distribution of the powder was then determined by analyzing SEM (scanning electron microscope) photographs. The measured particle radius distribution $N(R)$ and the distribution of the volume fraction $N(R)R^3$ are shown in Fig. 1.

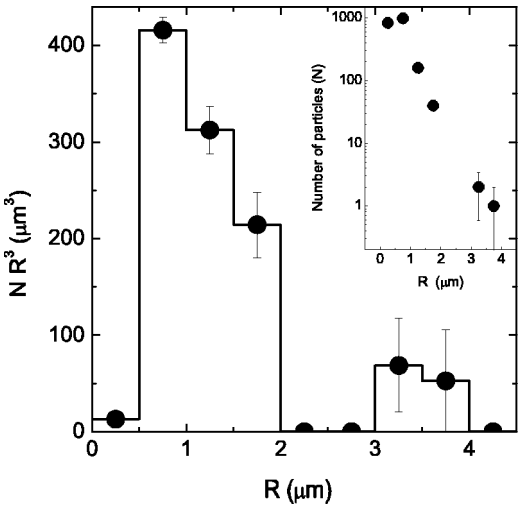

FIG. 1. The volume fraction distribution $N(R)R^3$ of $YBa_2Cu_4O_8$ sieved powder derived from the SEM photographs. The dashed line is the stepwise $G(R)$ function used for the $\lambda(T)$ determination by means of Eq. (8). The inset shows the grain size distribution $N(R)$. Errors are statistical.

The field-cooled (FC) dc-magnetization (M) measurements were performed with a Quantum Design SQUID magnetometer in a field of 0.5 mT for temperatures ranging from 5 K to 100 K. The absence of weak links between grains has been confirmed by the linear magnetic field dependence of the FC magnetization, measured at 0.25 mT, 0.5 mT, 0.75 mT and 1.0 mT for each pressure at $T=8$ K (see the inset in Fig. 2).

The hydrostatic pressure was generated in a copper-beryllium piston cylinder clamp that was especially designed

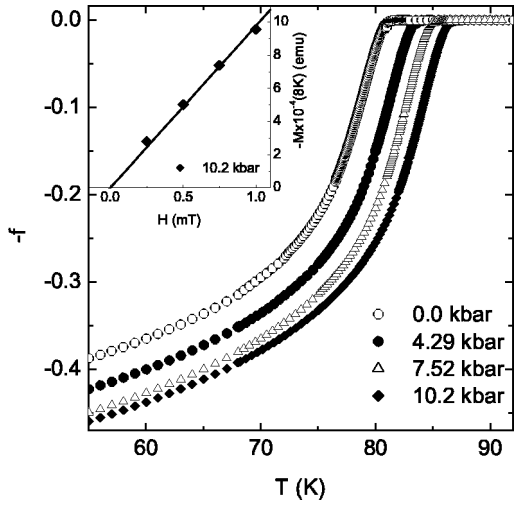

FIG. 2. The temperature dependence of the Meissner fraction f obtained from low-field (0.5 mT, FC) dc-magnetization measurements for various pressures. The inset shows $M(H)$ at $p=10.2$ kbar. Each point was measured after FC from $T>T_c$ to 8 K. The linear scale of M vs H data confirms the absence of the weak links between grains.

for magnetization measurements under pressure.[14] The sample was mixed with Fluorient FC77 (pressure transmitting medium) with a sample to liquid volume ratio of approximately 1/6. With this cell hydrostatic pressures up to 12 kbar can be achieved.[14] The pressure was measured *in situ* by monitoring the T_c shift of the small piece of In $[T_c(p=0)=3.4\ \mathrm{K}]$ included in the pressure cell.

B. Determination of the temperature dependence of λ from Meissner fraction measurements

The temperature dependence of λ^{-2} was extracted from the Meissner fraction f deduced from low-field (0.5 mT FC) magnetization data using the relation[15]

$$f(T)=\left(\frac{H}{M(T)}-N\right)^{-1}, \tag{7}$$

where H denotes the external magnetic field and N is the demagnetization factor. $N=1/3$ was taken assuming that the sample grains are spherical. Figure 2 shows the temperature dependence of the Meissner fraction close to T_c for different pressures. Three important features emerge: (i) The transition temperature T_c increases with increasing pressure. The value of $dT_c/dp=0.50(1)$ K/kbar is found, which is in good agreement with the literature data.[9–11] (ii) The value of f (Fig. 2) is much smaller than 1, confirming that the average grain size of the sample is compatible with λ. The reduction of f is caused by the field penetration at the surface of each individual grain for distances of the order of λ.[16] (iii) The absolute value of the Meissner fraction increases with pressure. Since the average grain size does not change under pressure and the grains are decoupled from each other, the rise of f must be attributed to a decrease of the magnetic penetration depth λ.

The temperature dependence of the penetration depth λ was analyzed from the measured $f(T)$ by using the Shoenberg formula[17] modified for the known grain size distribution:[18]

$$f(T)=\int_0^\infty\left(1-\frac{3\lambda(T)}{R}\coth\frac{R}{\lambda(T)}+\frac{3\lambda^2(T)}{R^2}\right)\times G(R)\mathrm{d}R\Big/\int_0^\infty G(R)\mathrm{d}R. \tag{8}$$

Here $G(R)=N(R)R^3$, and $N(R)$ is the grain size distribution (see Fig. 1). By solving this nonlinear equation, λ for each value of f was extracted, and then the set of $\lambda(T,p)$'s was reconstructed. Since the sample consists of an anisotropic nonoriented powder, the extracted λ is the so called effective penetration depth λ_{eff} (powder average). However, for sufficiently anisotropic extreme type II superconductors, including $YBa_2Cu_4O_8$, λ_{eff} is proportional to the in-plane penetration depth in terms of $\lambda_{eff}=1.31\lambda_{ab}$.[19] The resulting temperature dependence $\lambda_{ab}^{-2}(T,0)$ at ambient pressure is shown in Fig. 3. Note, that $\lambda_{ab}^{-2}(T)$ curves of the present work (see Fig. 3) are very similar to those reported in Ref. 20, obtained for $YBa_2Cu_4O_8$ using the same experimental technique. The fast increase of λ_{ab}^{-2} close to T_c and change of the linear slope at low temperatures in Ref. 20 was attributed to the contribution of the double chains to λ_{ab}^{-2}.

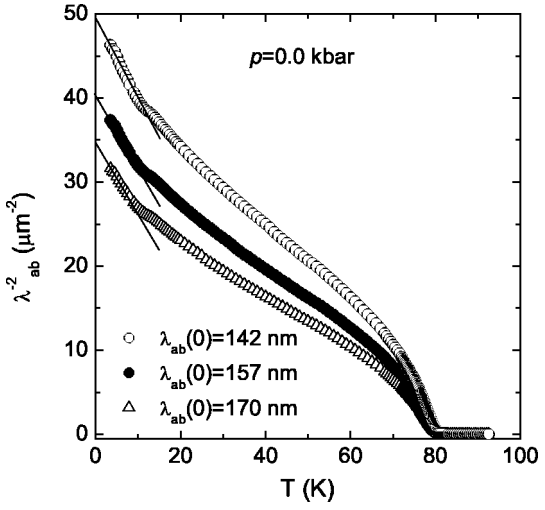

FIG. 3. The temperature dependence of λ_{ab}^{-2} for $YBa_2Cu_4O_8$ fine powder at ambient pressure calculated for different grain-size distribution functions. From top to bottom: $N^+(R)$, $N(R)$ and $N^-(R)$. The solid lines are the linear fits to the low-temperature behavior of $\lambda_{ab}^{-2}(T)$. The $\lambda_{ab}(0)$'s were obtained from the linear fits.

To estimate the error in the *absolute* value of $\lambda(0)$ introduced by the uncertainty in the grain-size distribution we performed reconstructions with two "extreme" conditions. For the first we took the grain-size distribution in the form $N^-(R)=N(R)-\sqrt{N(R)}$; for the second we took $N^+(R)=N(R)+\sqrt{N(R)}$. Appropriate $\lambda_{ab}^{-2}(T)$ dependencies for $N^+(R)$, $N(R)$ and $N^-(R)$ are shown in the inset of Fig. 3. The linear fit of the low temperature part of λ_{ab}^{-2} yields 142 nm for the lowest and 170 nm for the highest values of $\lambda(0)$. From these the absolute value of λ_{ab} can be estimated as $\lambda_{ab}(0)=156(14)$ nm that is in good agreement with the $\lambda_{ab}(0)$ obtained by means of μSR.[21–23]

Now we are turning to analyze the pressure dependence of λ_{ab}. As it was already mentioned, the procedure of the $\lambda^{-2}(T)$ reconstruction is sensitive to the grain-size distribution. The good thing here is that we study *relative* effects measured with the same sample in the same pressure cell, where most of the systematic errors are eliminated. The main systematic error for such measurements comes from misalignments of the experimental setup after the cell was removed from the SQUID magnetometer and put back again. We checked this procedure with a set of measurements at constant pressure. The systematic scattering of the magnetization data is of about 0.5%, giving a relative error in $\lambda^{-2}(T)$ of about 2%. Temperature dependencies of λ_{ab}^{-2} evaluated at different pressures are depicted in Fig. 4. The solid lines indicate the leading critical behavior of $\lambda_{ab}^{-2}(T)$ for homogenous and infinite domains,[1,24]

$$\lambda_{ab}^{-2}(T)=\lambda_{0ab}^{-2}|t|^{\nu}, \tag{9}$$

with $\nu\simeq 2/3$ in the 3D-XY universality class,[1,7] and the critical amplitude

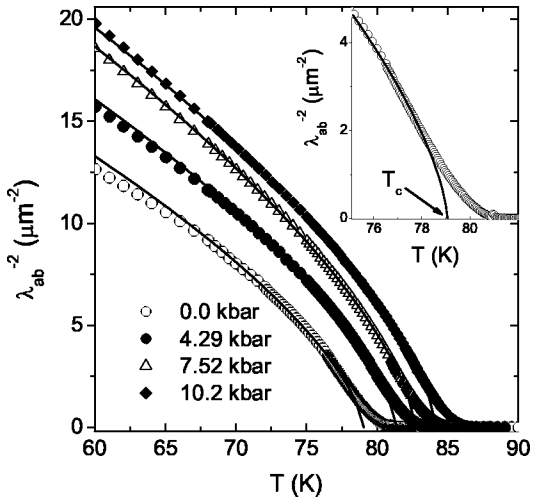

FIG. 4. The temperature dependence of λ_{ab}^{-2} for various pressures obtained from the $f(T)$ data (see Fig. 2) using Eq. (8). The solid lines indicate the leading critical behavior of a homogenous bulk system according to Eq. (9) with the parameters listed in Table I. The inset shows $\lambda_{ab}^{-2}(T)$ in the vicinity of T_c at ambient pressure. The deviations of the data points from the theoretical curves clearly uncover the finite-size behavior of the system.

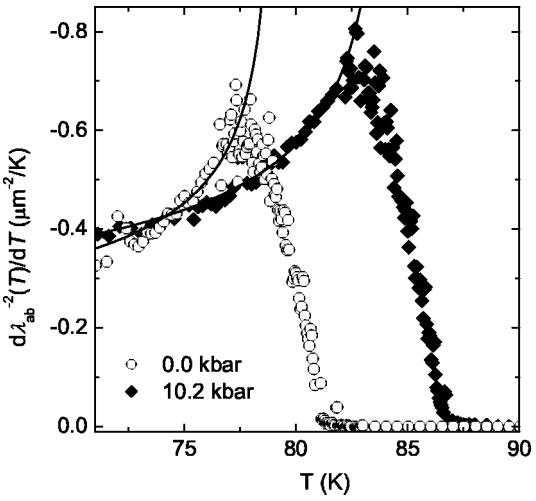

FIG. 5. $d\lambda_{ab}^{-2}(T)/dT$ vs T at different pressures. The maximum of $d\lambda_{ab}^{-2}(T)/dT$ is at a $T=T_{p_c}$. The solid lines are the corresponding derivatives of Eq. (9) indicating the leading behavior for a homogenous bulk system.

$$\lambda_{0ab}^{-2} = \frac{16\pi^3 k_B T_c}{\Phi_0^2 \xi_{0ab}^t}. \tag{10}$$

The values of λ_{0ab} and T_c obtained from the fit of Eq. (9) to the experimental data presented in Fig. 4 are summarized in Table I. Since Eq. (9) is valid in the vicinity of T_c only, we restricted the fit to the interval from T_c to T_c-10 K.

IV. THE FINITE-SIZE ANALYSIS

The essential characteristic of a homogeneous bulk cuprate superconductor is a sharp superconductor to normal state transition. A glance to the inset of Fig. 4 shows that in the samples considered here that is not the case. The transition occurs smoothly and there is a tail pointing to a finite-size effect associated with an inflection point at some characteristic temperature T_{p_c}. As outlined above [Eqs. (1) and (2)] at T_{p_c} the transverse correlation length ξ_{ab}^t attains the limiting length along the c-axis. To substantiate the occurrence of an inflection point we show in Fig. 5, $d\lambda_{ab}^{-2}(T)/dT$ versus T for $YBa_2Cu_4O_8$ samples at different pressures. The extreme in the first derivative of $\lambda_{ab}^{-2}(T)$ clearly reveals the existence of an inflection point at $T_{p_c}<T_c$. The absolute values of T_{p_c} obtained from a parabolic fit to experimental data around maximum point are summarized in Table I.

To substantiate the finite-size scenario further, we explore the scaling properties of the data with respect to the consistency with the finite-size scaling function. Noting that $\nu \simeq 2/3$ in the 3D-XY universality class,[1,7] Eq. (4) can be rewritten as

$$\frac{\lambda_{0ab}^2}{\lambda_{ab}^2}|t|^{-2/3} = g\left(\frac{t}{|t_{p_c}|}\right). \tag{11}$$

Figure 6(a) shows the resulting scaling function. For a comparison, we included the limiting behavior of the finite-size scaling function g_∞ [see Eq. (5)] for a homogeneous ($L_c \to \infty$) system [the solid line in Fig. 6(a)]. As it is seen, there is quite a good agreement between the experimental data and g_∞ function for t/t_{p_c} far from 0 (T far from T_c), whereas in the vicinity of 0 ($T \sim T_c$) the data are completely inconsistent with such a stepwise behavior. The experimental data have to diverge at $t/t_{p_c} \to 0$. As outlined in Sec. II divergence of the scaling function $g(t/|t_{p_c}|)$ at $t/t_{p_c} \to 0$ implies that the system is confined by a finite geometry. To strengthen this point we

TABLE I. Finite size estimates for T_{p_c}, λ_{0ab}^{-2}, $\lambda_{ab}^{-2}(T_{p_c})$ and the resulting relative shifts $\Delta T_{p_c}/T_{p_c}$ and $\Delta\lambda_{ab}^2(T_{p_c})/\lambda_{ab}^2(T_{p_c})$ for different pressures. L_{p_c} and $\Delta L_{p_c}/L_{p_c}$ are deduced from Eq. (3).

	T_c (K)	T_{p_c} (K)	λ_{0ab}^{-2} (μm^{-2})	$\lambda_{ab}^{-2}(T_{p_c})$ (μm^{-2})	L_c (Å)	$\frac{\Delta T_c}{T_c}$ (%)	$\frac{\Delta T_{p_c}}{T_{p_c}}$ (%)	$\frac{\Delta\lambda_{ab}^{-2}(T_{p_c})}{\lambda_{ab}^{-2}(T_{p_c})}$ (%)	$\frac{\Delta L_c}{L_c}$ (%)
0.0 kbar	79.07(1)	77.5(1)	34.3(7)	2.44(5)	50.8(1.0)	-	-	-	-
4.29 kbar	81.40(1)	79.7(1)	39.2(8)	2.92(6)	43.7(9)	2.95(2)	2.84(5)	19.7(2.8)	−14.0(3.0)
7.52 kbar	82.73(3)	81.1(1)	44.1(9)	3.29(7)	39.4(8)	4.63(4)	4.65(5)	34.8(2.8)	−22.4(3.0)
10.2 kbar	84.22(3)	82.5(1)	45.0(9)	3.36(7)	39.3(8)	6.51(4)	6.45(5)	37.7(2.8)	−22.6(3.0)

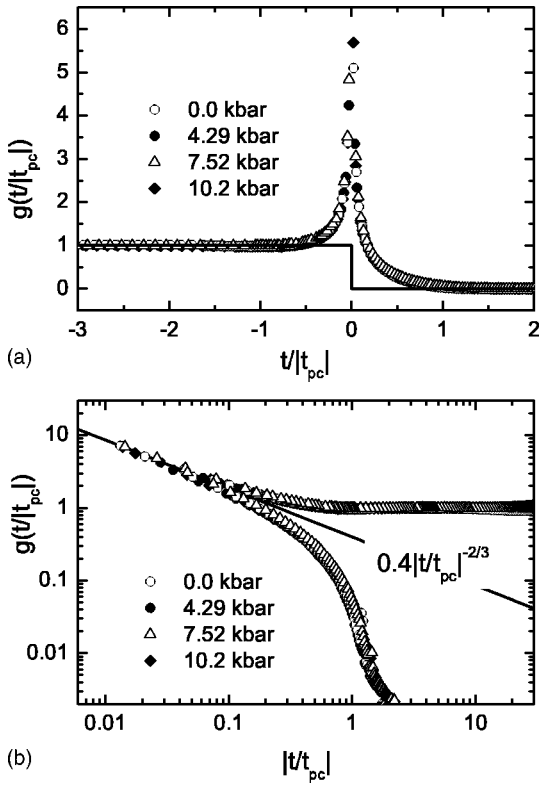

FIG. 6. Finite size scaling function g [Eq. (11)] versus $t/|t_{p_c}|$ (a) and versus $|t/t_{p_c}|$ in a logarithmic scale (b) for different pressures. The solid stepwise line in (a) is the g_∞ function for the homogenous ($L_c \to \infty$) system [see Eq. (5)]. The solid line in (b) is the leading finite-size behavior $g_{0c}|t/t_{p_c}|^{-2/3}$ at $t \to 0$ with $g_{0c}=0.40$ as it follows from Eq. (6).

display in Fig. 6(b) the comparison with the leading finite-size behavior $g_c(t \to 0)=g_{0c}|t/t_{p_c}|^{-2/3}$, as it is follows from Eq. (6). Noting that the amplitude g_{0c} depends on the shape of the domains and on the boundary conditions,[1] it is remarkable that the experimental data collapses on two branches. Accordingly, the shape of the domains and the boundary conditions on the interface do not change significantly under applied pressure. The straight line in Fig. 6(b) corresponds to $g_{0c} \simeq 0.40$. This value is compatible with $g_{0_c} \simeq 0.5$ found for $YBa_2Cu_3O_{6.7}$ oriented powder and for $Bi_2Sr_2CaCu_2O_{8+\delta}$ thin films.[1] Much larger values, $g_{0c} \approx 1.1-1.6$, have been found for $Bi_2Sr_2CaCu_2O_{8+\delta}$ single crystals[1] and for $Y_{1-x}Pr_xBa_2Cu_3O_{7-\delta}$ powders with $0.0 \leqslant x \leqslant 0.3$.[7]

To summarize, the finite-size scaling analysis of the in-plane penetration depth data for $YBa_2Cu_4O_8$ is fully consistent with a finite-size effect. Indeed we established the consistency with all three characteristics of a finite-size effect (see Sec. II). The finite-size estimates for λ_{0ab}^{-2} and $\lambda_{ab}^{-2}(T_{p_c})$ at different pressures are summarized in Table I.

V. THE PRESSURE DEPENDENCE OF THE DOMAIN SIZE

Using Eq. (3) and the estimates for T_{p_c} and $\lambda_{ab}^{-2}(T_{p_c})$ listed in Table I, the domain size L_c along the c-axis is readily

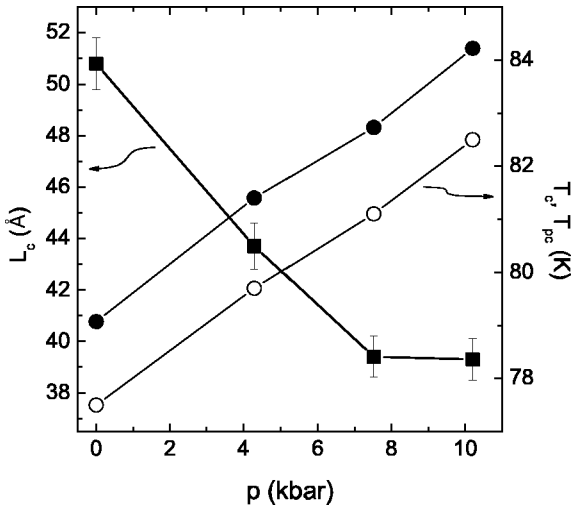

FIG. 7. The pressure dependence of L_c the domain size along the c-axis (■), transition temperature T_c (●), and inflection point temperature T_{p_c} (○) in $YBa_2Cu_4O_8$.

calculated. In Fig. 7 we display the pressure dependence of L_c, $T_c(p)$ and $T_{p_c}(p)$. It is seen that L_c decreases with pressure, whereas $T_c(p)$ and $T_{p_c}(p)$ increase almost linearly. On the other hand T_c and T_{p_c} increase with decreasing L_c. This agrees with the behavior found in $Y_{1-x}Pr_xBa_2Cu_3O_{7-\delta}$, where T_c and T_{p_c} were found to increase with reduced L_c.[7] Here T_c and T_{p_c} have been reduced by increasing the Pr content x. In this context it is interesting to note that in granular aluminum T_c was found to increase with reduced grain size.[25] Another striking feature is the nanoscale magnitude of L_c, even though $YBa_2Cu_4O_8$ is stoichiometric.

To check the consistency of our estimates we plot in Fig. 8 the relative shifts of T_{p_c}, $\lambda_{ab}^2(T_{p_c})$ and L_c versus the relative shift of T_c. According to Eq. (3) these shifts are not independent but related by

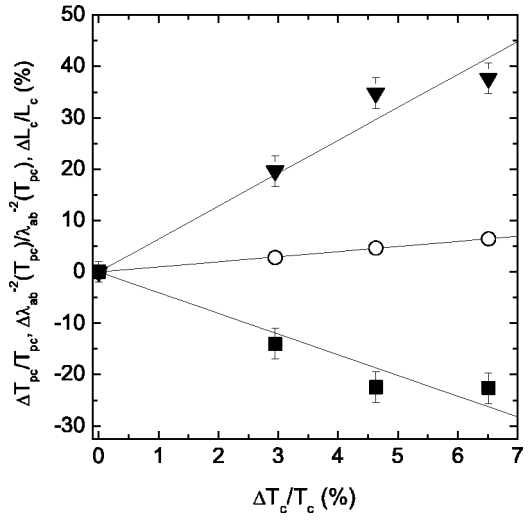

FIG. 8. The relative shifts of $\Delta\lambda_{ab}^{-2}(T_{p_c})/\lambda_{ab}^{-2}(T_{p_c})$ (▼); $\Delta L_c/L_c$ (■), and $\Delta T_{p_c}/T_{p_c}$ (○) vs the relative shift of $\Delta T_c/T_c$. The solid lines represent the linear fits with $\Delta L_c/L_c=-4.0(5)\cdot\Delta T_c/T_c$, $\Delta T_{p_c}/T_{p_c}=1.00(7)\cdot\Delta T_c/T_c$ and $\Delta\lambda_{ab}^{-2}(T_{p_c})/\lambda_{ab}^{-2}(T_{p_c})=6.4(5)\cdot\Delta T_c/T_c$.

$$\frac{\Delta L_c}{L_c} = \frac{\Delta T_{p_c}}{T_{p_c}} - \frac{\Delta \lambda_{ab}^{-2}(T_{p_c})}{\lambda_{ab}^{-2}(T_{p_c})}. \quad (12)$$

The straight lines correspond to the linear fits with $\Delta L_c/L_c = -4.0(5)\cdot\Delta T_c/T_c$, $\Delta T_{p_c}/T_{p_c} = 1.00(7)\cdot\Delta T_c/T_c$ and $\Delta\lambda_{ab}^{-2}(T_{p_c})/\lambda_{ab}^{-2}(T_{p_c}) = 6.4(5)\cdot\Delta T_c/T_c$, revealing that Eq. (12) is almost satisfied. Furthermore, these estimates show that the reduction of L_c with pressure reflects the fact that the pressure effect on $\lambda_{ab}^{-2}(T_{p_c})$ exceeds the effect on T_c considerably. Having established the consistency of our estimates it is essential to recognize that the occurrence of nanoscale superconducting domains is not an artefact of $YBa_2Cu_4O_8$ and our samples. Indeed the existence of nanoscale domains has been established in a variety of cuprates, including films, powders and single crystals.[1,6–8]

VI. CONCLUSION

To summarize, we reported the observation of combined finite-size and pressure effects on the lengths L_c of the superconducting domains along the *c*-axis and the in-plane penetration depth λ_{ab} in a cuprate superconductor. The evidence for a finite-size behavior of the system stems from the tail in $\lambda_{ab}^{-2}(T)$ observed in the vicinity of T_c. We have shown that the scaling properties of the tail are fully consistent with a finite-size effect, arising from domains with nanoscale size along the *c*-axis. Indeed the essential characteristics of a finite-size effect, as (i) the limiting properties of the scaling function $g(t/|t_{p_c}|)$, (ii) the existence of an inflection point in $\lambda^{-2}(T)$ and (iii) the extremum in $d\lambda^{-2}(T)/dT$ at T_{p_c} have been verified. Even though $YBa_2Cu_4O_8$ is *stoichiometric* we have shown that the size of the domains along the *c*-axis is of nanoscale only, ranging from 50.8(1.0) Å to 39.3(8) Å at pressures from 0.0 to 10.2 kbar. This raises serious doubts on the existence of macroscopic phase coherent superconductivity. Contrary-wise, this does not exclude a percolative resistive superconductor to normal state transition, when the superconducting domains percolate. Indeed, a granular superconductor is usually characterized by two parameters:[26] the first is the domain's size and the second the coupling between them. The coupling is accomplished randomly with a temperature dependent probability. Such a mechanism is a percolation process; at the temperature where the coupling probability is equal to the percolation threshold, an infinite cluster of coupled superconducting grains is formed. This suggests that resistive bulk superconductivity is achieved by a percolative process, while the phase coherent superconducting properties and the spatial extent of the domains can be probed by thermal fluctuations and finite-size effects.

The authors are grateful to J. Roos for stimulating discussions, K. Conder for help during sample preparation and T. Strässle for providing pressure cell for magnetization measurements. This work was supported by the Swiss National Science Foundation and by the NCCR program Materials with Novel Electronic Properties (MaNEP) sponsored by the Swiss National Science Foundation.

*Electronic address: rustem.khasanov@psi.ch

[1] T. Schneider and D. Di Castro, Phys. Rev. B **69**, 024502 (2003).
[2] J. Mesot, P. Allenspach, U. Staub, A. Furrer, and H. Mutka, Phys. Rev. Lett. **70**, 865 (1993); A. Furrer, P. Allenspach, F. Fauth, M. Guillaume, W. Henggeler, J. Mesot, and S. Rosenkranz, Physica C **235–240**, 261 (1994).
[3] N. Alekseevskii, I. Garifullin, N. Garif'yanov, B. Kochelaev, A. Mitin, V. Nizhankovskii, L. Tagirov, G. Khaliullin, and E. Khlybov, JETP Lett. **48**, 37 (1988).
[4] J. X. Liu, J. C. Wan, A. M. Goldman, Y. C. Chang, and P. Z. Jiang, Phys. Rev. Lett. **67**, 2195 (1991); A. Chang, Z. Y. Rong, Y. M. Ivanchenko, F. Lu, and E. L. Wolf, Phys. Rev. B **46**, 5692 (1992); T. Cren, D. Roditchev, W. Sacks, J. Klein, J.-B. Moussy, C. Deville-Cavellin, and M. Laguës, Phys. Rev. Lett. **84**, 147 (2000); K. M. Lang, V. Madhavan, J. E. Hoffman, E. W. Hudson, H. Eisaki, S. Uchida, and J. C. Davis, Nature (London) **415**, 412 (2002).
[5] D. Di Castro, G. Bianconi, M. Colapietro, A. Pifferi, N. L. Saini, S. Agrestini, and A. Bianconi, Eur. Phys. J. B **18**, 617 (2000).
[6] T. Schneider, cond-mat/0210702.
[7] T. Schneider, R. Khasanov, K. Conder, and H. Keller, J. Phys.: Condens. Matter **15**, L763 (2003).
[8] T. Schneider, J. Supercond. **17**, 41 (2003).
[9] J. J. Scholtz, E. N. van Eenige, R. J. Wijngaarden, and R. Griessen, Phys. Rev. B **45**, 3077 (1992).
[10] B. Bucher, J. Karpinski, E. Kaldis, and P. Wachter, Physica C **157**, 478 (1989).
[11] E. N. van Eenige, R. Griessen, R. J. Wijngaarden, J. Karpinski, E. Kaldis, S. Rusiecki, and E. Jilek, Physica C **168**, 482 (1990).
[12] N. Schultka and E. Manousakis, Phys. Rev. B **52**, 7528 (1995).
[13] K. Conder, Ch. Krüger, E. Kaldis, D. Zech, and H. Keller, Physica C **225**, 13 (1994).
[14] T. Strässle, Ph.D. thesis, ETH Zürich, 2002.
[15] S. Blundell, *Magnetism in Condensed Matter* (Oxford University Press, Oxford, 2001).
[16] G. M. Zhao, M. B. Hunt, H. Keller, and K. A. Müller, Nature (London) **385**, 236 (1997).
[17] D. Shoenberg, Proc. R. Soc. London, Ser. A **175**, 49 (1940).
[18] A. Porch, J. R. Cooper, D. N. Zheng, J. R. Waldram, A. M. Campbell, and P. A. Freeman, Physica C **214**, 350 (1993).
[19] V. I. Fesenko, V. N. Gorbunov, and V. P. Smilga, Physica C **176**, 551 (1991).
[20] C. Panagopoulos, J. L. Tallon, and T. Xiang, Phys. Rev. B **59**, R6635 (1999).
[21] R. Khasanov, D. Di Castro, D. G. Eshchenko, D. Andreica, K. Conder, S. Kazakov, J. Karpinski, E. Pomjakushina, I. M. Savić, R. Tetean, and H. Keller, in preparation.
[22] H. Keller, W. Kündig, I. M. Savić, H. Simmler, B. Stäuble-Pümpin, M. Warden, D. Zech, P. Zimmermann, E. Kladis, J. Karpinski, S. Rusiecki, J. H. Brewer, T. M. Riseman, J. W. Schneider, Y. Maeno, and C. Rossel, Physica C **185–189**, 1089 (1991).

[23] C. Bernhard, Ch. Niedermayer, U. Binniger, A. Hofer, Ch. Wenger, J. L. Tallon, C. V. M. Williams, E. J. Ansaldo, and J. I. Budnick, Phys. Rev. B **52**, 10 488 (1995).

[24] T. Schneider and J. M. Singer, *Phase Transition Approach To High Temperature Superconductivity* (Imperial College Press, London, 2000).

[25] G. Deutscher *et al.*, J. Low Temp. Phys. **10**, 231 (1973).

[26] G. Deutscher, O. Entin-Wohlman, S. Fishman, and Y. Shapira, Phys. Rev. B **21**, 5041 (1980).